# Homogeneous Nucleation in Supercritical Fluids

When a supercritical solution is rapidly expanded, large solute supersaturations can be attained, and small particles are formed. The evolution of the homogeneous nucleation rate, work of nucleus formation, and critical nucleus size along different expansion paths is investigated here for the model system phenanthrene-carbon dioxide. Nucleation rates are the result of the competition among solvent expansion, cooling due to depressurization, and high supersaturation. Although supersaturations can reach very high values ($>10^6$), relatively flat nucleation rate profiles result due to cooling and expansion. For an interfacial tension of 0.02 N/m, computed nucleation rates never exceed $10^4\ s^{-1} \cdot cm^{-3}$. A substantial fraction of the maximum nucleation rate is attained with partial decompression to pressures above 1 bar.

**Pablo G. Debenedetti**
Department of Chemical Engineering
Princeton University
Princeton, NJ 08544

## Introduction

The formation of solids following the rapid expansion of supercritical solutions offers considerable promise as a means for the production of thin films, crystalline or amorphous powders with narrow and controllable particle size distribution, and intimate mixtures of amorphous materials (Matson et al., 1987a). This process is, accordingly, of potential interest in applications ranging from ceramic precursor processing, production of polymeric microspheres for chromatography packings and controlled drug delivery, and as an alternative to milling in the pharmaceutical industry.

In this method of solids processing, the substance of interest, generally a nonvolatile solute, is first dissolved in a supercritical fluid. In the relative vicinity of the solvent's critical point, the resulting dilute solution is characterized by a high compressibility. Small changes of pressure give rise to large changes in density (and hence solvent power) (Kumar and Johnston, 1988). The expansion of the original solution, consequently, results in the precipitation of the dissolved solute. Although the starting mixture is liquid-like in density, its high compressibility allows nucleation to be triggered mechanically (pressure reduction) rather than thermally. Mechanical perturbations travel at the speed of sound, favoring the rapid attainment of uniform conditions within the expanding fluid. Dilute mixtures of nonvolatile solutes in supercritical solvents, furthermore, are frequently characterized by high enhancement factors (ratio of actual solubility to the same quantity, as predicted assuming ideal gas behavior at the prevailing temperature and pressure). The rapid expansion of supercritical mixtures can therefore result in very high supersaturations. This combination of large supersaturation and uniform conditions favors small particles and narrow size distributions, and is a distinguishing feature of this process.

To date, work on solids formation by expansion of supercritical solutions has been exclusively experimental (Krukonis, 1984; Larson and King, 1986; Petersen et al., 1986; Matson et al., 1986a,b, 1987a,b; Mohamed et al., 1989a,b; Halverson, 1989; Chang and Randolph, 1989; Tavana and Randolph, 1989; see Mohamed et al., 1989a for a detailed discussion).

The commercial application of this promising technology, henceforth referred to as RESS (rapid expansion of supercritical solutions) (Matson et al., 1987a) depends in part upon a sound understanding of the underlying physical phenomena. This means taking into consideration the processes of particle formation and growth (nucleation, condensation, coagulation; see, for example, Gelbard et al., 1980; Friedlander, 1983; Warren and Seinfeld, 1985; Turner et al., 1988; Pratsinis, 1988), as well as nonidealities peculiar to supercritical solutions, which can give rise to an inversion in the sign of the solute's heat of condensation (Chimowitz and Pennisi, 1986; Chimowitz et al., 1988; Debenedetti and Kumar, 1988). In addition, nucleation, condensation and coagulation take place in a fluid medium with unusual thermophysical properties (for example, liquid-like density coupled with compressibility in excess of its ideal gas value; viscosity intermediate between gas and liquid-like). In the vicinity of the solvent's critical point, furthermore, physical properties are very sensitive to small changes in temperature and pressure. Although the phenomena involved are well understood individually, their interaction makes this problem particularly interesting.

The formation of monodisperse aerosols by vapor condensation in nozzles is a well known process (Turner et al., 1988). Optimal nozzle and expansion conditions for RESS, however, have not been investigated to date. Most RESS experiments (e.g., Mohamed et al., 1989a,b; Chang and Randolph, 1989) have been performed under conditions approaching free expansion following flow through a narrow restriction. Under these conditions, most of the expansion happens after the restriction (Matson et al., 1987a). This situation is best described by free jet expansion models (e.g., Murphy and Miller, 1984). Nevertheless, a continuous RESS process involving only partial expansion is attractive, since it would reduce solvent recompression costs and would allow greater control over the product size distribution (Tavana and Randolph, 1989). In this mode of operation, the mixture would be expanded in a subsonic converging nozzle into a chamber held at a convenient pressure, and the solvent recirculated after mechanical separation of the powder. It is, therefore, very important to understand whether appreciable nucleation rates can be achieved with partial expansions. Consequently, in this paper, we investigate an important aspect of the full RESS problem, exploring the evolution of the nucleation rate along different expansion paths. All calculations are for phenanthrene in carbon dioxide.

## Energetics

The type of system considered here consists of a nonvolatile solid solute dissolved in a supercritical solvent, and exhibits so-called attractive behavior (Debenedetti and Mohamed, 1989). Solubility enhancement in such systems (i.e., ratio of actual to ideal-gas-predicted solubility at the same temperature and pressure) can be as high as $10^6$. The phase behavior of attractive mixtures of nonvolatile solutes in supercritical solvents has been extensively discussed elsewhere (McHugh and Krukonis, 1986; Kim et al., 1985; Rowlinson and Swinton, 1982). For the systems and process conditions of interest here, solvent dissolution in the solid precipitate is negligible. Furthermore, since solvent condensation upon expansion leads to recrystallization (Mohamed et al., 1989a; Chang and Randolph, 1989) and is therefore undesirable, the expansions considered in this work are into the solvent's single-phase region. The process considered here is thus one in which pure solute nuclei are formed within the supercritical solution.

The minimum work associated with the formation of a nucleus of $n$ molecules of a single-component isotropic phase (e.g., liquid) within a different single-component bulk phase (e.g., vapor) can be written as (Reiss, 1970; Katz and Blander, 1973)

$$W_{\min} = (P - P')V' + \sigma F + [\mu'(P', T) - \mu(T, P)]n \quad (1)$$

where $F$ denotes the nucleus' surface area, $\sigma$, the interfacial tension, $V'$, the nucleus' volume, $P'$, the pressure inside the nucleus, and $P$, the pressure in the bulk phase (i.e., $\mu'$ is the chemical potential inside the isotropic nucleus). For an incompressible nucleus, such as we consider here,

$$\mu'(P', T) - \mu'(P, T) = v'(P' - P) \quad (2)$$

where $v'$ is the molecular volume of the condensed phase, which does not depend on pressure. Then,

$$n[\mu'(P', T) - \mu'(P, T)] = V'(P' - P) \quad (3)$$

Substituting this expression for $V'(P - P')$ into Eq. 1 and defining

$$\Delta\mu = \mu'(P, T) - \mu(P, T) \quad (4)$$

we obtain

$$W_{\min} = \sigma F + n\Delta\mu \quad (5)$$

where $\Delta\mu$ is now the difference in chemical potentials between the two phases, but at the bulk temperature and pressure (Gibbs, 1877; Frenkel, 1955). We now consider a dilute solution of a nonvolatile solute (1) in a supercritical fluid (2). For a nucleus containing only solute molecules, Eq. 5 reads

$$W_{\min} = \sigma F + n[\mu_1^s(T, P) - \mu_1(T, P, y_1)] \quad (6)$$

where $W_{\min}$ now denotes the minimum work associated with the formation of a nucleus of $n$ solute particles within a bulk solution of pressure $P$, temperature $T$, and solute mole fraction $y_1$, $\mu_1^s(T, P)$ is the chemical potential of the pure solid solute at $T$ and $P$, and $\mu_1(T, P, y_1)$, its chemical potential in the fluid phase. Let $y_1^e(T, P)$ denote the equilibrium (saturation) solute mole fraction in the supercritical fluid. At equilibrium, the solute's chemical potentials in the solid and fluid phases are equal,

$$\mu_1^s(T, P) = \mu_1(T, P, y_1^e) \quad (7)$$

and Eq. 6 can be written as

$$W_{\min} = \sigma F + n[\mu_1(T, P, y_1^e) - \mu_1(T, P, y_1)] \quad (8)$$

The solute's chemical potential is given by

$$\mu_1 = kT \ln Py_1\phi_1 + \lambda_1(T) \quad (9)$$

where $\phi_1$ is the solute's fugacity coefficient. For dilute solutions, we can write

$$\phi_1 = \phi_1^\infty \exp(-Ky_1) \quad (10)$$

where $K$ is only a function of temperature and pressure, and $\phi_1^\infty$ is the solute's fugacity coefficient at infinite solution (Debenedetti and Kumar, 1986). Using this expression for the solute's fugacity coefficient, the difference in chemical potentials in Eq. 8 reads

$$\mu_1(T, P, y_1^e) - \mu_1(T, P, y_1) = kT \ln \frac{y_1^e \exp(-Ky_1^e)}{y_1 \exp(-Ky_1)} \quad (11)$$

or equivalently,

$$\mu_1(T, P, y_1^e) - \mu_1(T, P, y_1) = kT\left[\ln\left(\frac{y_1^e}{y_1}\right) - Ky_1^e\left(1 - \frac{y_1}{y_1^e}\right)\right] \quad (12)$$

Substituting Eq. 12 into Eq. 8, we obtain

$$W_{\min} = \sigma F + nkT[Ky_1^e(S - 1) - \ln S] \tag{13}$$

where $S$ denotes the supersaturation $(y_1/y_1^e)$. If the fluid phase behaves as an ideal gas mixture $(\phi_1 = 1)$ or as an ideal solution $[\phi_1 = \phi_1(T, P)]$, we recover the familiar expression,

$$W_{\min} = \sigma F - nkT \ln S \tag{14}$$

Since, for given $T$ and $P$, the solution is stable $(y_1 \leq y_1^e)$ or metastable $(y > y_1^e)$ but not unstable, we must have

$$\left(\frac{\partial \mu_1}{\partial y_1}\right)_{T,P} > 0 \tag{15}$$

or equivalently,

$$1 + \left(\frac{\partial \ln \phi_1}{\partial \ln y_1}\right)_{T,P} > 0 \tag{16}$$

which implies, in addition to $Ky_1^e < 1$,

$$S < (Ky_1^e)^{-1} \tag{17}$$

Assuming the nucleus to be spherical, its critical size is given by

$$n^* = \frac{32\pi}{3}\left[\frac{\sigma v_1^{2/3}}{kT}\right]^3\left[\frac{1}{\ln S - Ky_1^e(S - 1)}\right]^3 \tag{18}$$

$$r^* = 2\left[\frac{\sigma v_1}{kT}\right]\left[\frac{1}{\ln S - Ky_1^e(S - 1)}\right] \tag{19}$$

where $n^*$ and $r^*$ denote the number of solute molecules in, and radius of, the nucleus, for which the function $W_{\min}(n)$ is maximized, and $v_1$ is the molecular volume of the solid solute.

When $S > 1$, the fluid phase is metastable. Critical nuclei, on the other hand, are unstable: smaller nuclei disappear, and bigger nuclei grow (Frenkel, 1955; Gibbs, 1877). Thus, the critical nucleus is simply a threshold size that must be reached before a phase transition can occur. Since the thermodynamic treatment is limited to the onset of a phase transition, it provides no information on the progress of such an event beyond its initial, embryonic stage represented by the fluctuation-dominated formation of nuclei (Lifshitz and Pitaevskii, 1981).

## Kinetics

The nucleation rate expression used in this paper is based on classical nucleation theory (Becker and Doring, 1935; Zeldovich, 1942; Frenkel, 1955; Lifshitz and Pitaevskii, 1981). Several excellent reviews of this topic are available (Springer, 1978; McDonald, 1962, 1963; Blander and Katz, 1975; Seinfeld, 1986; Friedlander, 1977). A detailed derivation of the rate expression can be found in the Appendix.

Classical nucleation theory arrives at a rate expression through thermodynamic (equilibrium) considerations. It is based on several approximations: those whose validity is unchanged by operation under typical RESS conditions are discussed in the Appendix. Here, we investigate whether two of the theory's key assumptions retain their validity during RESS.

### *Diluteness*

The concentration of nuclei is assumed to be small and the solute is assumed to exist overwhelmingly as single molecules ($n = 1$; "monomer"). This allows one to postulate that the growth or breakdown of nuclei occurs via elementary steps consisting of the attachment or loss of single solute molecules. Given the almost liquid-like density of supercritical solvents, it is natural to inquire as to the validity of this picture under typical RESS conditions. Using $10^{-2}$ mol/cm$^3$ as a representative solvent density and a solute mole fraction of $10^{-3}$, we obtain a solute concentration of $10^{-5}$ mol/cm$^3$. For comparison, there are $4 \times 10^{-5}$ mol/cm$^3$ in an ideal gas at 1 bar and 300 K. Thus, it is reasonable to assume that the mixture is, in this sense, dilute.

Results of recent fluorescence spectroscopy experiments (Brennecke and Eckert, 1989) have shown that pyrene can form excimers (excited state dimers) at very low mole fractions when the solvent is close to its critical point. At present, it is not known whether these strong solute-solute interactions occur in all dilute supercritical systems or only in certain specific mixtures. The assumption of an unassociated solute, therefore, needs to be critically examined as knowledge on this question progresses.

### *Steady state*

Since rapid expansion is an essential feature of the process, the use of a rate expression derived for steady-state conditions needs to be critically examined. Several authors have addressed the "time lag" question (Zeldovich, 1942; Kantrowitz, 1951; Wakeshima, 1954; Probstein, 1951; Andres and Boudart, 1965; Collins, 1955; Feder et al., 1966). This is the name given to the characteristic relaxation time required to establish a time-invariant (but nonequilibrium) population of clusters. As discussed by Springer (1978), the time lag predicted by Wakeshima (1954), Collins (1955), and Feder et al. (1966) can be written as

$$\tau^{-1} \approx \frac{2aPyv_1^s}{kT}\sqrt{\frac{\sigma}{2\pi m}} \tag{20}$$

where $\tau$ is the time lag, $a$ is a numerical constant which differs from theory to theory [i.e., $a = 4$ according to Collins (1955); $a = 2$ according to Feder et al (1966); $a = 8\pi$ according to Wakeshima (1954)], $m$ is the solute's mass, and the other quantities have already been defined. Since we are concerned that $\tau$ may be too large, we must use the worst possible (i.e., smaller) value for $a$. Taking $a$ to be unity, and using $v_1 = 3 \times 10^{-28}$ m$^3$ (molecular volume of solid phenanthrene); $kT = 4.39 \times 10^{-21}$ kg · m$^2$/s$^2$ (318 K); $\sigma = 0.04$ N/m; $m = 2.96 \times 10^{-25}$ kg (mass of a phenanthrene molecule), we obtain

$$\tau(s) = \frac{4.99 \times 10^{-10}}{P(\text{bar})y} \tag{21}$$

At 200 bar and $y = 10^{-3}$, this yields a time lag of $2 \times 10^{-9}$ s. On the other hand, for $P = 15$ bar and $y = 10^{-5}$, the time lag becomes $3 \times 10^{-6}$ s. These estimates must be compared with typical RESS expansion times, which range from $10^{-6}$ to $10^{-5}$ s (Matson et al., 1987a; Mohamed et al., 1989a). Therefore, the steady-state assumption is an accurate picture of reality during the initial stages of the expansion and a plausible approximation that needs to be carefully checked on a case-by-case basis once the supercritical solvent has expanded significantly. Equations 20 and 21 apply to condensation coefficients (i.e., fraction of molecules which condense from those hitting the surface of a nucleus) equal to unity. Otherwise, Eq. 20 should be multiplied by $\xi$, the condensation coefficient. Since this number can range from 0.04 to 1 (Springer, 1978), the preceding considerations should be interpreted with caution, and time lag estimates should not be given more than qualitative significance.

In what follows we assume that the solute exists primarily as single molecules and that the time lag is much shorter than the expansion time, so that steady-state conditions corresponding to any given temperature, pressure, and supersaturation are established "instantaneously." Then, as shown in the Appendix, we obtain the following rate expression

$$I = 2N_{\text{tot}}\beta\sqrt{\frac{\sigma v_1^2}{kT}} \cdot \exp\left\{-\frac{16\pi}{3}\left(\frac{\sigma v_1^{2/3}}{kT}\right)^3\left[\frac{1}{\ln S - Ky_1^e(S-1)}\right]^2\right\} \quad (22)$$

where $\beta$ is the thermal flux of solute molecules, i.e., $\beta = Py_1/\sqrt{2\pi mkT}$ for ideal gas behavior, and $N_{\text{tot}}$ is the solute's concentration in the supercritical fluid.

Equation 22 gives the number of critical nuclei formed per unit time in a unit volume. It describes events occurring over a time span which is short compared to that required for an appreciable decrease in the existing supersaturation to occur. Since the underlying theory treats nuclei as macroscopic objects, it should be used with caution if calculated $n^*$ values are small. The thermodynamic expressions for $W_{\min}$, $r^*$, and $n^*$ apply, strictly speaking, to an isotropic (amorphous) solid (Gibbs, 1877). A rigorous treatment of homogeneous nucleation of crystalline materials is complicated by the fact that $\sigma$ is dependent upon the orientation of the surface planes relative to the solid's internal stresses. As is customary in discussions of homogeneous nucleation involving solids (Seinfeld, 1986; O'Hara and Reid, 1973; Kodas et al., 1986), $\sigma$ will be used as a parameter without altering the form of the equations. Note that $\sigma$ is the interfacial tension between the supercritical fluid and the solid solute. This quantity does not exhibit singularities and does not vanish at the solvent's critical point or at the lower critical end point.

## Effect of Fluid-Phase Nonideality

Solubility enhancement, retrograde behavior, and other characteristic features of the thermodynamics of dilute supercritical mixtures are a consequence of fluid-phase nonidealities. These are accounted for through the term $Ky_1^e(S - 1)$ in Eqs. 13, 18, 19, and 22. Even though the mixtures of interest here are dilute, the quantity $K$ can become very large and cannot be neglected *a priori* (Debenedetti and Kumar, 1986).

Note that fluid-phase nonideality enters into the picture through the $\Delta\mu$ term in Eq. 5. For single-component condensation or boiling, this situation has been addressed by Katz and Blander (1973), who treated the gas phase as an ideal mixture of clusters. In the present case, mixture nonideality is accounted for through $\phi_1$.

Figure 1 shows the behavior of $K$ for phenanthrene in $CO_2$ [$T_c = 304.2$ K; $P_c = 73.8$ bar] at two slightly supercritical temperatures. Analogous calculations for benzoic acid in $CO_2$ yielded very similar results (Debenedetti and Kumar, 1986). It can be seen that, in the relative vicinity of the solvent's critical point, $K$ becomes very large. This quantity has been given a molecular-based interpretation by Cochran and Lee (1987).

Calculations leading to Figure 1 were performed using the Peng-Robinson equation of state, with an interaction coefficient 0.1 (Peng and Robinson, 1976). For each condition of temperature and pressure, the composition range [$0 < y_1 < 0.1y_1^e(T, P)$] was divided into 100 intervals; at each composition, $\ln \phi_1$ was calculated, and $K$ was obtained by linear regression from the resulting $\ln \phi_1$ vs. $y_1$ line (see Eq. 10).

Figure 2 shows the pressure dependence of the supersaturation at the limit of stability, estimated as $1/(Ky_1^e)$, for phenanthrene in $CO_2$ at two slightly supercritical temperatures. All calculations in this paper were performed with the Peng-Robinson equation of state. It can be seen that fluid-phase nonideality limits the attainable range of supersaturations. Since the mixture becomes unstable when $S = (Ky_1^e)^{-1}$ (see Eq. 17), the increase in $K$ (Figure 1) and $y_1^e$ (solubility enhancement) imposes, in principle, a severe bound on the maximum amount of solute that can be present in a supercritical fluid before the onset of instability. Unless the solvent is cooled by expansion, nucleation will take place before supersaturations as high as those shown in Figure 2 can occur. If the supersaturation limits shown in Figure 2 are exceeded (which could conceivably occur at the higher pressures, where the allowable supersaturations are low), spinodal decomposition could occur. This interesting possibility has not been explored to date.

As the mixture expands, ideal behavior is approached, and no thermodynamic limits exist on the allowable supersaturation. Thus, Figure 2 is of interest at high pressure. The use of $1/K$ as an estimate for the limit of stability implies that the mixture is sufficiently dilute throughout, so that Eq. 10 applies (Debenedetti and Kumar, 1986). In the present case, $1/K$ values at supercritical pressures are never greater than 0.02.

Figure 3 shows the behavior of the work ($W_{\min}/kT$) required to form a spherical nucleus of $n$ solute molecules for phenanthrene in supercritical carbon dioxide. An interfacial tension of 0.04 N/m has been assumed. The "ideal" curve was calculated with $\ln S$ as the driving force for nucleation; the "actual" curve,

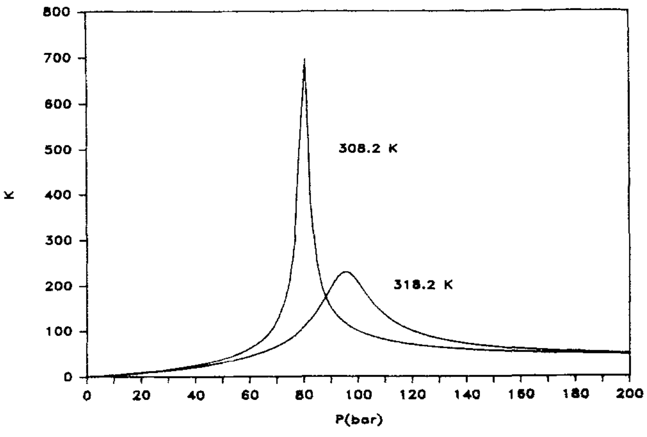

Figure 1. Dependence of $K$ upon pressure.

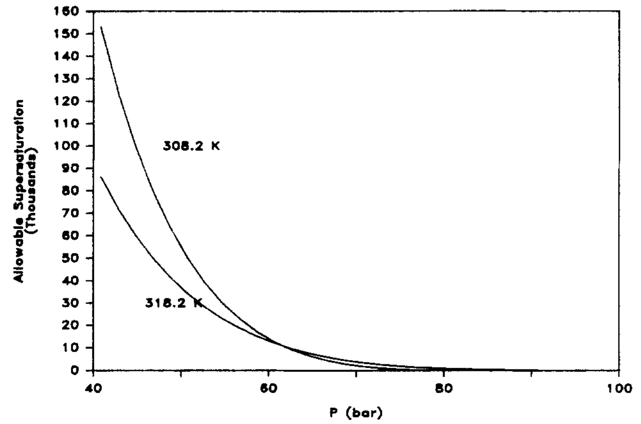

Figure 2. Supersaturation at the limit of stability, $(Ky_1^e)^{-1}$.

with $Ky_1^e(S - 1) - \ln S$ (see Eqs. 13 and 14). The values of $S$ (12.63), $K$ (99.39), and $y_1^e$ ($7.96 \times 10^{-4}$) used in the figure correspond to the limit of stability at 120 bar and 318.2 K [$S = (Ky_1^e)^{-1}$]. Although the effect of fluid-phase nonideality on the work of nucleus formation and on the size of the critical nucleus is seen to be significant ($n^* = 142$ vs. $n^* = 549$), it is the actual nucleation rate that one is ultimately interested in calculating. We now investigate the behavior of the homogeneous nucleation rate under typical RESS operating conditions.

## Attainable Nucleation Rate

We consider three possible expansion paths: (a) isothermal decompression from 200 bar to 1 bar at 318.2 K; (b) isobaric preheating at 121.6 bar from 318.2 K to 362.2 K, followed by isenthalpic expansion to 1 bar (and 253.2 K); and (c) isobaric preheating at 141.9 bar from 318.2 K to 362.2 K, followed by isentropic expansion to 121.6 bar (and 353.2 K) and subsequent isenthalpic expansion to 1 bar (and 227.2 K). In each case, the starting mixture is saturated.

The isothermal path is highly idealized and could be approximated by depressurizing a well-stirred autoclave with conducting walls immersed in a constant temperature bath. Preheating followed by isenthalpic expansion corresponds to steady adiabatic flow through a throttling valve into an atmospheric line, preceded by a heating section in which the fluid's temperature is raised enough to avoid solvent liquefaction (or solidification) upon expansion. The pre- and post-expansion conditions are isenthalpic only if changes in kinetic energy are negligible, a condition that is readily attained for large enough downstream tube diameters. (In the present example, the expansion from 121.6 bar and 362.2 K to 1 bar and 253 K is accompanied by a 125-fold density decrease; for 0.32 cm tubing upstream, and 1.9 cm tubing downstream, this brings about a 12-fold increase in kinetic energy; for a flow rate of 0.5 std. L/min through the restriction, the upstream velocity in 0.32 cm tubing is 7.4 mm/s, and, therefore, the change in kinetic energy is 0.004 $m^2/s^2$, which is entirely negligible.) The actual expansion process is complex, and involves shocks if the flow is choked in the restriction. This situation has been analyzed qualitatively by Matson and coworkers (Matson et al., 1987a) who considered free expansion of the jet into a large chamber after throttling. The present calculations, which assume isenthalpic conditions throughout the expansion (rather than simply between end states) are therefore an idealization. The last path differs from the isenthalpic case in that initial expansion (after preheating) takes place in a converging nozzle. Expansion calculations for the pure solvent were performed using actual $CO_2$ data (Perry et al., 1963; Raznjevic, 1976; Reynolds, 1979); all points are in the single-phase region. Symbols in Figures 4–9 denote those points whose temperature and pressure were read from thermodynamic charts.

At a given $T$ and $P$, the supersaturation is given in what follows by $y_1^e(T_i, P_i)/y_1^e(T, P)$, where $T_i$ and $P_i$ denote the initial conditions prior to expansion (i.e., $T_i = 318.2$ K, $P_i = 200$ bar for isothermal decompression). Thus, we calculate the maximum attainable nucleation rate for a given initial condition. Since no solute condensation is allowed in the present calculations, the expansion path is that of the pure solvent. The solute mole fraction never exceeds $2.6 \times 10^{-3}$ in the examples considered here; in more concentrated systems, the mixture's expansion path can differ from that of the pure solvent. At every temperature and pressure considered in the expansion calculations, the $K$ values calculated in the dilute limit were always within 5% of the value obtained by least squares fitting the $\ln \phi_1$ vs. $y_1$ relationship up to the maximum solute mole fraction used here ($2.6 \times 10^{-3}$).

Figure 4 shows the evolution of the maximum attainable

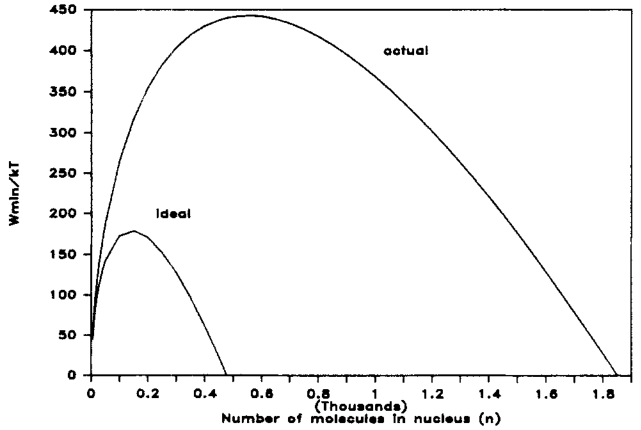

Figure 3. Work of formation of a spherical nucleus.

$P = 120$ bar; $T = 318.2$ K; $S = (Ky_1^e)^{-1} = 12.63$; $\sigma = 0.04$ N/m

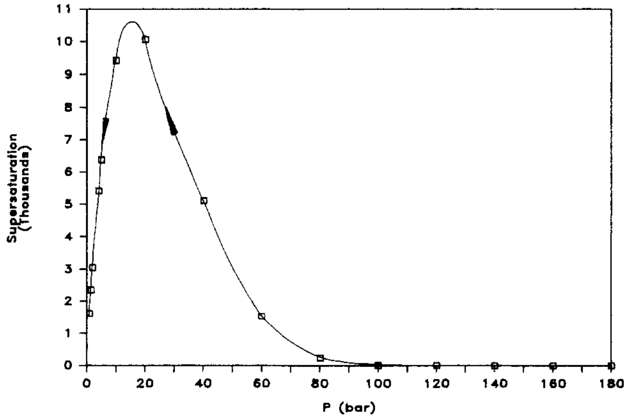

Figure 4. Attainable supersaturations: isothermal expansion at 318.2 K.

supersaturation as an initially saturated solution of phenanthrene at 318.2 K and 200 bar is decompressed isothermally to atmospheric pressure. Since the starting composition is fixed, the attainable supersaturation curve is inversely proportional to the solubility. Attainable supersaturations are also shown in Figure 5 for the isenthalpic and isentropic-isenthalpic cases, respectively. As will be shown below, both the solvent's expansion (which lowers the solute's concentration) and the consequent temperature drop give rise to relatively flat nucleation rate profiles even in the presence of supersaturations as exceptionally large as those shown in Figure 5.

For the three expansion paths considered here, the difference between $\ln S$ and $\ln S - Ky_1^e(T, P)(S - 1)$ (i.e., the ideal and real driving forces for nucleation) was never greater than 24%. On the other hand, if an initially saturated mixture of phenanthrene in carbon dioxide at 160 bar and 318 K were rapidly expanded isothermally to 80 bar, the ideal and real driving forces at the latter condition would be very different: 3.05 and 1.73, respectively. In general, nonideality tends to be more important ($K$ greater) during the initial stages of the expansion, when supersaturations (and hence nucleation rates) are small. This cancellation tends to decrease the effect of mixture nonideality upon the computed nucleation rate. This effect, however, will always be significant close enough to criticality.

Figure 6 shows the attainable nucleation rate as an initially saturated mixture of phenanthrene in carbon dioxide is decompressed from 200 bar to atmospheric pressure while the temperature is maintained at 318.2 K. Labels on the curves in Figures 6–9 are interfacial tensions in N/m, and the nucleation rates are in $\mathrm{cm}^{-3} \cdot \mathrm{s}^{-1}$. The nucleation rate was calculated with Eq. 22, using the ideal gas value for the thermal flux ($\beta$) and the Peng-Robinson equation to compute the solute's concentration at the given temperature, pressure, and mole fraction. Errors arising from using the ideal-gas value for $\beta$ (but with the actual pressure, $P$) are relatively minor when compared with the effects of uncertainties in interfacial tension upon the calculated nucleation rates. Nevertheless, the derivation of expressions for $\beta$, which take into account solvent nonideality and strong solute-solvent interactions (clustering; Petsche and Debenedetti, 1989), is an important question that needs to be addressed. Solvent expansion, on the other hand, plays a major role in RESS, and it is important to use the actual solvent concentration at a given temperature and pressure to calculate $N_{\mathrm{tot}}\ (= y_1 \times N_{\mathrm{solvent}})$.

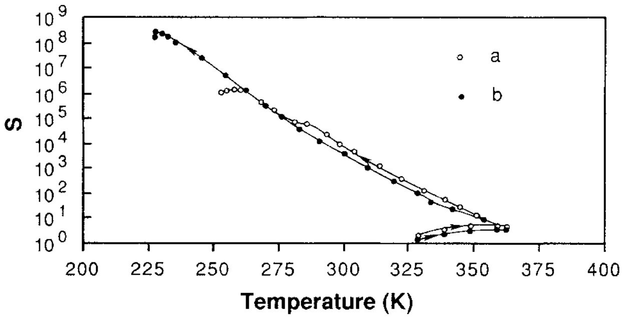

**Figure 5. Attainable supersaturations: a. isobaric preheat, isenthalpic expansion; b. isobaric preheat, isentropic, and then isenthalpic expansion.**

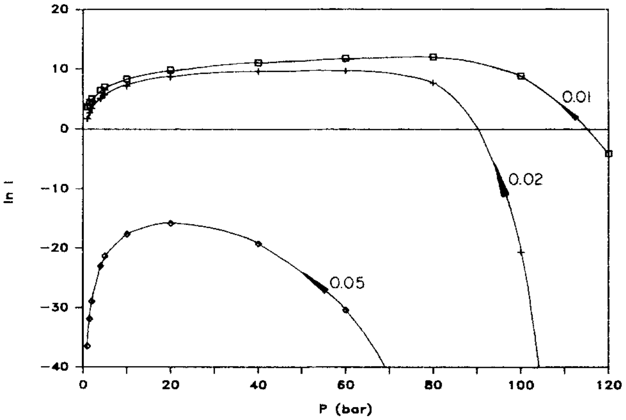

**Figure 6. Attainable nucleation rates for different interfacial tensions (N/m): isothermal expansion at 318.2 K.**

For $\sigma = 0.02$ N/m, the attainable nucleation rate increases by 12 orders of magnitude between 100 and 80 bars. Thereafter, there is a rough balance between increase in the thermodynamic driving force and decrease in solute concentration, with the attainable rate remaining at roughly $10^4\ \mathrm{cm}^{-3}\mathrm{s}^{-1}$. This balance is remarkable: one would not, in general, expect a preexponential factor (solute concentration) to compete with an exponential term (the supersaturation). In RESS, however, the solvent's compressibility, which is very large near the critical point, gives rise to very large changes in solute concentration with moderate changes in pressure.

The calculations leading to Figure 6 should be interpreted with caution. Their objective is to illustrate those aspects of the problem which are unique to RESS, and not to predict actual nucleation rates. In order for this to be possible, independent estimates of the interfacial tension must be available. Since there is considerable experimental evidence of homogeneous nucleation in the free-expansion RESS configuration used by Halverson (1989) and Mohamed et al. (1989a,b), the present calculations suggest that typical values for $\sigma$ between organic solids and supercritical solvents should be around 0.02 N/m; the calculations along different expansion paths presented below confirm this estimate. Furthermore, the calculated critical nuclei for the low and intermediate surface tensions lose their macroscopic character (upon which the whole theory is based) around 100 bars and become O(1) quantities upon further expansion. This is shown in Figure 7. Under these conditions, rate predictions based on thermodynamic arguments retain qualitative significance, but cannot be considered predictive.

Figure 8 shows rate calculations for the isenthalpic expansion. The initial portion along each curve corresponds to the isobaric preheating. Because the mixture exhibits retrograde solubility under these conditions (i.e., solubility decreases as temperature increases; see, for example, Debenedetti and Kumar, 1988), preheating can give rise to appreciable nucleation for low enough interfacial tensions. Even though the isenthalpic expansion gives rise to very large attainable supersaturations (see Figure 5), attainable nucleation rates are not significantly greater than in the isothermal expansion case (compare Figures 6, 8). This is because of the large temperature drop along the isenthalpic path.

Attainable nucleation rates along the isentropic-isenthalpic

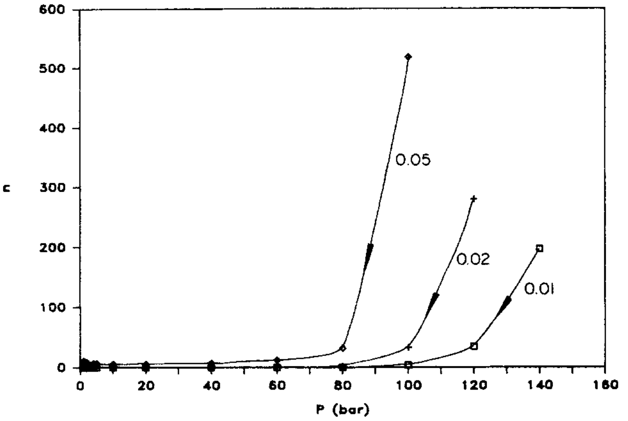

**Figure 7. Number of molecules in a critical nucleus for different interfacial tensions (N/m): isothermal expansion at 318.2 K.**

path (following preheat) are shown in Figure 9. The trends are qualitatively similar to those exhibited during isenthalpic expansion.

## Discussion

In this paper, we have investigated the predictions of classical nucleation theory regarding the behavior of the work of formation of a critical nucleus, the size of the critical nucleus, and the nucleation rate, along three possible expansion paths relevant to RESS processing. The application of classical nucleation theory to RESS involves no additional approximation other than the ones made routinely in aerosol calculations (Warren and Seinfeld, 1985; Pratsinis, 1988; Turner et al., 1988).

The calculations take into account fluid-phase nonideality. They address the limiting situation wherein the solute's mole fraction in the expanding fluid remains constant at its initial value. Thus, the calculated supersaturations and nucleation rates represent the highest possible values consistent with the particular initial conditions and expansion paths.

Attainable rates along the different expansion paths explored here exhibit some common characteristics. In the first place, fluid-phase expansion plays a key role. This is a consequence of the solvent's large compressibility and tends to cause a significant decrease in nucleation rate with only moderate changes in pressure. Secondly, although attainable supersaturations can reach very large values (Figure 5), this is accompanied by a large temperature decrease. The interaction between these competing effects (pronounced decrease in solute concentration due to solvent expansion; increase in attainable supersaturation; temperature drop) tends to give rise to relatively flat attainable nucleation rate profiles. For the system investigated here and an assumed surface tension of 0.02 N/m, maximum rates do not exceed $10^4$ per ($cm^3 \cdot s$) for both the isenthalpic and isentropic-isenthalpic paths.

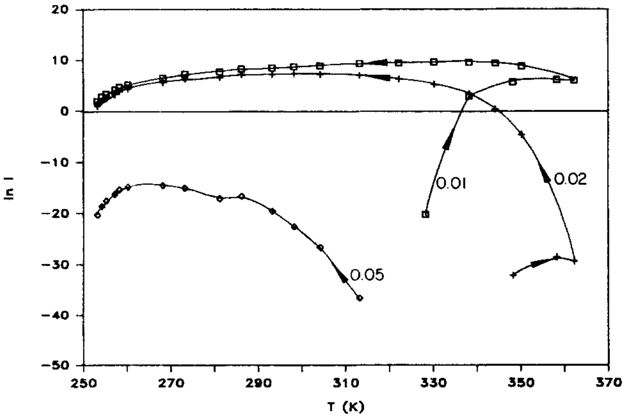

**Figure 8. Attainable nucleation rates for different interfacial tensions (N/m): isobaric preheat, isenthalpic expansion.**

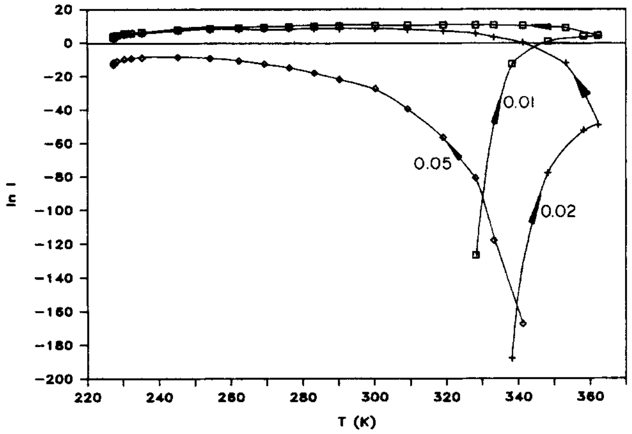

**Figure 9. Attainable nucleation rates for different interfacial tensions (N/m): isobaric preheat, isentropic, and then isenthalpic expansion.**

An appreciable fraction of the maximum nucleation rate can be achieved in all cases after partial expansion. Thus, for a surface tension of 0.02 N/m, a nucleation rate of 2,200 $cm^{-3} \cdot s^{-1}$ is attained at 80 bar for the isothermal expansion (maximum, 15,800 $cm^{-3} \cdot s^{-1}$ at 60 bar); along the isenthalpic path, the nucleation rate becomes 1,100 $cm^{-3} \cdot s^{-1}$ at 51 bar (maximum, 1,300 $cm^{-3} \cdot s^{-1}$ at 35.5 bar); along the isentropic-isenthalpic path, the nucleation rate becomes 1,400 $cm^{-3} \cdot s^{-1}$ at 71 bar (maximum, 5,700 $cm^{-3} \cdot s^{-1}$ at 35.5 bar). Thus, the concept of partial expansion (Tavana and Randolph, 1989) appears feasible.

The conditions and physical properties used in the present calculations are representative of relatively small organic solutes ($MW < 10^3$), processed with solvents having moderate critical temperatures (approximately 300 K) and are of interest, for example, in RESS processing of pharmaceutical compounds (Mohamed et al., 1989a). In other situations, such as the production of inorganic powders from supercritical water (Matson et al., 1987a,b), the operating temperature ranges are very different from the ones considered here, and the conclusions derived in this paper will not apply.

Our calculations represent just the first step towards a quantitative understanding of RESS. The full mathematical description must account for particle growth (aerosol dynamics) and for the coupling among mass, energy, and momentum balances in the highly nonideal fluid phase. Finally, the need for "measurements" (e.g., from carefully controlled nucleation expeeriments) and estimation techniques for interfacial tensions between solids and supercritical fluids cannot be overstated.

## Acknowledgment

The author gratefully acknowledges the financial support of the National Science Foundation (Grant CBT 8657010), the donors of the Petroleum Research Fund, administered by the American Chemical Society, the Camille and Henry Dreyfus Foundation for a 1989 Teacher-Scholar Award; Merck, Sharp and Dohme Research Laboratories, and Enzytech, Inc., of Cambridge, MA. The author is also grateful to a referee for suggesting the possibility of spinodal decomposition in the RESS process.

## Notation

$a$ = numerical constant defined in Eq. 20
$F$ = surface area of a nucleus, $L^2$
$f$ = nucleus distribution function, $L^{-3}$
$I$ = nucleation rate, $t^{-1} \cdot L^{-3}$
$K$ = function of temperature and pressure defined in Eq. 10
$k$ = Boltzmann's constant, $1.38 \times 10^{-23}$ J/K
$m$ = mass of a solute molecule, M
$N_{tot}$ = total solute concentration in the bulk fluid phase, $L^{-3}$
$n$ = number of molecules in a nucleus
$P$ = pressure, $ML^{-1} \cdot t^{-2}$
$r$ = radius of a spherical nucleus, L
$S$ = supersaturation ratio
$T$ = temperature, $\theta$
$v_1$ = molecular volume of solid solute, $L^3$
$W_{min}$ = reversible work of nucleus formation, $ML^2 \cdot t^{-2}$
$y$ = mole fraction

### *Greek letters*

$\alpha$ = convective coefficient for nucleus flux in size space, $t^{-1}$
$\beta$ = thermal flux of solute molecules, $t^{-1} \cdot L^{-2}$
$\delta$ = diffusive coefficient for nucleus flux in size space, $t^{-1}$
$\gamma$ = evaporative flux, $L^{-2} \cdot t^{-1}$
$\phi$ = fugacity coefficient
$\lambda$ = function of temperature defined in Eq. 9, $ML^2 \cdot t^{-2}$
$\mu$ = chemical potential, $ML^2 \cdot t^{-2}$
$\sigma$ = interfacial tension, $Mt^{-2}$
$\tau$ = lag time, t

### *Superscripts*

$e$ = equilibrium
$s$ = solid
$'$ = inside the nucleus
$*$ = critical nucleus
$\infty$ = infinite dilution

### *Subscripts*

1 = solute
$\circ$ = metastable equilibrium

## Literature Cited

Andres, R. P., and M. Boudart, "Time Lag in Multistate Kinetics: Nucleation," *J. Chem. Phys.*, **42**, 2057 (1965).

Becker, R., and W. Doering, "Kinetische Behandlung der Keimbildung in Ubersettigten Dampfen," *Ann Phys.*, Leipzig, **24**, 719 (1935).

Blander, M., and J. L. Katz, "Bubble Nucleation in Liquids," *AIChE J.*, **21**, 833 (1975).

Brennecke, J. F., and C. A. Eckert, "Fluorescence Spectroscopy Studies of Intermolecular Interactions in Supercritical Fluids," *Supercritical Fluid Science and Technology*, K. P. Johnston and J. M. L. Penninger, eds., *ACS Symp. Ser.*, **406**, Chap. 2 (1989).

Chang, C. J., and A. D. Randolph, "Precipitation of Microsize Organic Particles from Supercritical Fluids," *AIChE J.*, **35**, 1876 (1989).

Chimowitz, E. H., and K. Pennisi, "Process Synthesis Concepts for Supercritical Gas Extraction in the Crossover Region," *AIChE J.*, **32**, 1665 (1986)

Chimowitz, E. H., F. D. Kelley, and F. M. Munoz, "Analysis of Retrograde Behavior and the Crossover Effect in Supercritical Solvents," *Fluid Phase Equil.*, **44**, 23 (1988).

Cochran, H. D., and L. L. Lee, "General Behavior of Dilute Binary Solutions," *AIChE J.*, **34**, 170 (1988).

Collins, F. C.,. "Time Lag in Spontaneous Nucleation due to Nonsteady State Effects," *Z. Elektrochem.*, **59**, 404 (1955).

Debenedetti, P. G., and S. K. Kumar, "Infinite Dilution Fugacity Coefficients and the General Behavior of Dilute Binary Systems," *AIChE J.*, **32**, 1253 (1986).

———, "The Molecular Basis of Temperature Effects in Supercritical Extraction," *AIChE J.*, **34**, 645 (1988).

Debenedetti, P. G., and R. S. Mohamed, "Attractive, Weakly Attractive, and Repulsive Near-Critical Systems," *J. Chem. Phys.*, **90**, 4528 (1989).

Feder, J., K. C. Russell, J. Lothe, and G. M. Pound, "Homogeneous Nucleation and Growth of Droplets in Vapors," *Adv. Phys.*, **15**, 111 (1966).

Frenkel, J., *Kinetic Theory of Liquids*, Chap. 7, Dover, New York (1955).

Friedlander, S. K., *Smoke, Dust, and Haze: Fundamentals of Aerosol Behavior*, Chs. 8 and 9, Wiley-Interscience, New York (1977).

———, "Dynamics of Aerosol Formation by Chemical Reaction," *Ann. N.Y. Acad. Sci.*, **404**, 354 (1983).

Gelbard, F., Y. Tambour, and J. H. Seinfeld, "Sectional Representations for Simulating Aerosol Dynamics," *J. Colloid Interf. Sci.*, **76**, 541 (1980).

Gibbs, J. W., "On the Equilibrium of Heterogeneous Substances," *Trans. Conn. Acad. Sci.*, **III**, 108 (Oct., 1875–May, 1876); 343 (May, 1877–July, 1878).

Halverson, D. S.,. *Precipitation from Supercritical Fluids: Effects of Process Conditions on the Morphology and Particle Size of Precipitation Products*, MS Thesis, Princeton Univ. (1989).

Kantrowitz, A., "Nucleation of Very Rapid Vapor Expansions," *J. Chem. Phys.*, **19**, 1097 (1951).

Katz, J. L., and M. Blander, "Condensation and Boiling: Corrections to Homogeneous Nucleation Theory for Nonideal Gases," *J. Colloid Interf. Sci.*, **42**, 496 (1973).

Kim, S., J. M. Wong, and K. P. Johnston, "Theory of the Pressure Effect in Dense Gas Extraction," *Supercritical Fluid Technology*, J. M. L. Penninger, M. Radosz, M. McHugh, and V. Krukonis, eds., Elsevier, Amsterdam, 45 (1985).

Kodas, T. T., S. E. Pratsinis, and S. K. Friedlander, "Aerosol Formation and Growth in a Laminar Core Reactor," *J. Colloid Interf. Sci.*, **111**, 102 (1986).

Krukonis, V., "Supercritical Fluid Nucleation of Difficult-to-Comminute Solids," paper 140f, AIChE meeting, San Francisco (Nov., 1984).

Kumar, S. K., and K. P. Johnston, "Modeling the Solubility of Solids in Supercritical Fluids with Density as an Independent Variable," *J. of Supercrit. Fluids*, **1**, 15 (1988).

Larson, K. A., and M. L. King, "Evaluation of Supercritical Fluid Extraction in the Pharmaceutical Industry," *Biotech. Prog.*, **2**, 73 (1986).

Lifshitz, E. M., and L. P. Pitaevskii, *Physical Kinetics*, Vol. 10, Chap. 12, *Course of Theoretical Physics*, L. D. Landau and E. M. Lifshitz, Pergamon, Oxford (1981).

Matson, D. W., R. C. Petersen, and R. D. Smith, "Formation of Silica Powders from the Rapid Expansion of Supercritical Solutions," *Adv. Cer. Mat.*, **1**, 242 (1986a).

———, "The Precipitation of Polycarbosilane Powders and Fibers During Rapid Expansion of Supercritical Fluid Solutions," *Mat. Lett.*, **4**, 429 (1986b).

Matson, D. W., J. L. Fulton, R. C. Petersen, and R. D. Smith, "Rapid Expansion of Supercritical Fluid Solutions: Solute Formation of Powders, Thin Films, and Fibers," *Ind. Eng. Chem. Res.*, **26**, 2298 (1987a).

Matson, D. W., R. C. Petersen, and R. D. Smith, "Production of Fine Powders by the Rapid Expansion of Supercritical Fluid Solutions," *Adv. in Ceram.*, **21**, 109 (1987b).

McDonald, J. E., "Homogeneous Nucleation of Vapor Condensation: I. Thermodynamic Aspects," *Amer. J. Phys.*, **30,** 870 (1962).

———, "Homogeneous Nucleation of Vapor Condensation: II. Kinetic Aspects," *Amer. J. Phys.*, **31,** 31 (1963).

McHugh, M., and V. J. Krukonis, *Supercritical Fluid Extraction: Principles and Practice,* Butterworths, Boston (1986).

Mohamed, R. S., D. S. Halverson, P. G. Debenedetti, and R. K. Prud'homme, "Solids Formation after the Expansion of Supercritical Mixtures," *ACS Symp. Ser.,* No. 406, Chap. 23, *Supercritical Science and Technology,* K. P. Johnston and J. M. L. Penninger, eds., 355 (1989a).

Mohamed, R. S., P. G. Debenedetti, and R. K. Prud'homme, "Effects of Process Conditions on Crystals Obtained from Supercritical Mixtures," *AIChE J.*, **35,** 325 (1989b).

Murphy, H. R., and D. R. Miller, "Effects of Nozzle Geometry on Kinetics in Free-Jet Expansions," *J. Phys. Chem.*, **88,** 4474 (1984).

O'Hara, M., and R. C. Reid, *Modeling Crystal Growth from Solution,* Prentice-Hall, Englewood Cliffs, NJ (1973).

Peng, D. Y., and D. B. Robinson, "A New Two-Constant Equation of State," *Ind. Eng. Chem. Fundam.*, **15,** 59 (1976).

Perry, R. H., C. H. Chilton, and S. K. Kirkpatrick, eds., *Chemical Engineers' Handbook,* 4th ed., McGraw-Hill, New York (1963).

Petsche, I. B., and P. G. Debenedetti, "Solute-Solvent Interactions in Infinitely Dilute Supercritical Mixtures: a Molecular Dynamics Investigation," *J. Chem. Phys.*, **91,** 7075 (1989).

Petersen, R. C., D. W. Matson, and R. D. Smith, "Rapid Precipitation of Low Vapor Pressure Solids from Supercritical Fluid Solutions: the Formation of Thin Films and Powders," *J. Amer. Chem. Soc.*, **108,** 2100 (1986).

Pratsinis, S., "Simultaneous Nucleation, Condensation, and Coagulation in Aerosol Reactors," *J. Colloid Interf. Sci.*, **124,** 416 (1988).

Probstein, R. F., "Time Lag in Self Nucleation of a Supersaturated Vapor," *J. Chem. Phys.*, **19,** 619 (1951).

Raznjevic, K., *Handbook of Thermodynamic Tables and Charts,* McGraw-Hill, New York (1976).

Reiss, H., "Treatment of Droplike Clusters by Means of the Classical Phase Integral in Nucleation Theory," *J. Stat. Phys.*, **2,** 83 (1970).

Reynolds, W. C., *Thermodynamic Properties in SI,* Dept. of Mechanical Engineering, Stanford Univ. (1979).

Rowlinson, J. S., and F. L. Swinton, *Liquids and Liquid Mixtures,* 3rd ed., Butterworths, London (1982).

Seinfeld, J. H., *Atmospheric Chemistry and Physics of Air Pollution,* Chap. 9, Wiley-Interscience, New York (1986).

Springer, G. S., "Homogeneous Nucleation," *Adv. Heat Transf.*, **14,** 281 (1978).

Tavana, A., and A. D. Randolph, "Manipulating Solids CSD in a Supercritical Fluid Crystallizer: $CO_2$-Benzoic Acid," *AIChE J.*, **35,** 1625 (1989).

Turner, J. R., T. K. Kodas, and S. K. Friedlander, "Monodisperse Particle Production by Vapor Condensation in Nozzles," *J. Chem. Phys.*, **88,** 457 (1988).

Wakeshima, H., "Time Lag in Self Nucleation," *J. Chem. Phys.*, **22,** 1614 (1954).

Warren, D. R., and J. H. Seinfeld, "Simulation of Aerosol Size Distribution Evolution in Systems with Simultaneous Nucleation, Condensation, and Coagulation," *Aerosol Sci. Tech.*, **4,** 31 (1985).

Zeldovich, J., "Theory of Nucleation and Condensation," *Sov. Phys. JETP,* Eng. Transl., **12,** 525 (1942).

## Appendix

The derivation of an expression for the nucleation rate follows classical nucleation theory arguments (Becker and Doring, 1935; Zeldovich, 1942; Frenkel, 1955; Lifshitz and Pitaevskii, 1981). We consider nuclei to be large objects ($n$ large), and their concentration to be small, so that the solute exists overwhelmingly as "monomer" ($n = 1$). Then, the growth or breakdown of nuclei occurs via elementary steps consisting of the attachment or loss of single solute molecules. The evolution of the nucleus distribution function then satisfies the Fokker-Planck equation,

$$\frac{\partial f}{\partial t} = -\frac{\partial I}{\partial n} \tag{A1}$$

where $f(n, t)dn$ is the number of nuclei per unit volume within the size range $[n, n + dn]$ at time $t$, and $I(n)$ is the net rate (per unit volume) at which $n$-mers (nuclei containing $n$ molecules) are formed by monomer condensation onto $(n - 1)$-mers, minus the rate at which they are destroyed by monomer evaporation. Since the rate can be regarded as a flux in nucleus size space, we can write

$$I = -\delta\frac{\partial f}{\partial n} + \alpha f \tag{A2}$$

where the two terms represent the diffusional and convective contributions to the flux in size space.

For $n < n^*$, nuclei are distributed according to

$$f_\circ(n) \propto \exp\left[-W_{\min}(n)/kT\right] \tag{A3}$$

where subscript $\circ$ denotes the "equilibrium" distribution. Here, equilibrium denotes the state of the metastable fluid over times smaller than the characteristic time for the formation of a critical nucleus (Lifshitz and Pitaevskii, 1981). Accordingly, Eq. A3 is only meaningful for $n < n^*$. Since no work is needed to form a single-particle nucleus and we have assumed that the solute exists overwhelmingly as single molecules, the proportionality constant in Eq. A3 is of the order of $N_{\text{tot}}$, the total solute concentration. Upon setting $I = 0$ for $f = f_\circ$, we obtain the relationship between the diffusive and convective coefficients in Eq. A2,

$$\alpha = -\frac{\delta}{kT}\frac{dW_{\min}}{dn} \tag{A4}$$

At steady state, $I$ becomes independent of $n$,

$$-\delta\frac{\partial f}{\partial n} - \frac{\delta f}{kT}\frac{dW_{\min}}{dn} = I = \text{const.} \tag{A5}$$

In addition,

$$\frac{df_\circ}{dn} = -\frac{f_\circ}{kT}\frac{dW_{\min}}{dn} \tag{A6}$$

so that Eq. A5 can be rearranged to read

$$-\delta f_\circ \frac{\partial(f/f_\circ)}{\partial n} = I \tag{A7}$$

Now, for small $n$, $f$ and $f_\circ$ are indistinguishable. This means that the metastable fluid acts as a reservoir for small nuclei, their inventory being replenished so fast as to make their distribution indistinguishable from the "equilibrium" case (Lifshitz and Pitaevskii, 1981). For $n > n^*$, $f_\circ$ (which then has only matheical significance) increases without bounds, whereas $f$ is necessarily finite (or vanishing). Thus,

$$\lim_{n\to 0}\frac{f}{f_o} = 1 \tag{A8}$$

$$\lim_{n\to\infty}\frac{f}{f_o} = 0 \tag{A9}$$

Equation A9 does not imply the physical existence of an "equilibrium" distribution of nuclei for $n > n^*$; it provides a closure condition for the calculation of the rate, $I$:

$$I = \left[\int_0^\infty \frac{dn}{\delta f_o}\right]^{-1} \tag{A10}$$

It follows from the definition of $I$ that

$$I(n) = f(n-1)\beta F(n-1) - f(n)\gamma F(n) \tag{A11}$$

and

$$f_o(n-1)\beta F(n-1) = f_o(n)\gamma F(n) \quad (n < n^*) \tag{A12}$$

where $F(n)$ is the surface area of a nucleus containing $n$ molecules. The simultaneous validity of Eqs. A11 and A12 implies that the characteristic time for the attainment of an equilibrium velocity distribution is much smaller than that associated with the formation of a critical nucleus.

Combining Eqs. A11 and A12, we obtain

$$I(n) = f_o(n-1)F(n-1)\beta\left[\frac{f(n-1)}{f_o(n-1)} - \frac{f(n)}{f_o(n)}\right] \tag{A13}$$

which, in the macroscopic limit ($n$ = large) becomes

$$I(n) = -f_o(n)F(n)\beta\frac{\partial(f/f_o)}{\partial n} \tag{A14}$$

Comparison with Eq. A7 yields

$$\delta = \beta F(n) \tag{A15}$$

Substituting Eq. A15 into Eq. A10, and expanding $f_o$ about $n^*$,

$$\frac{I}{\beta F(n^*)}\int_{-\infty}^{\infty} \cdot \frac{d(\Delta n)}{N_{\mathrm{tot}}\exp\left[-\frac{W_{\min}(n^*)}{kT} - W''_{\min}(*)\frac{(\Delta n)^2}{2kT}\right]} = 1 \tag{A16}$$

where $\Delta n = n - n^*$, $W''_{\min}(*)$ denotes the second derivative of $W_{\min}(n)$, evaluated at the (unstable) equilibrium condition (i.e., $n = n^*$), and we have used the sharpness of the integrand's peak at equilibrium to factor $F(n)$ out of the integral at its equilibrium value, as well as to transform the limits of integration from $[n \ll n^*; n \gg n^*]$ to $[-\infty; +\infty]$. Then, using Eq. 13 and assuming the nucleus to be spherical we obtain

$$I = 2N_{\mathrm{tot}}\beta\sqrt{\frac{\sigma v_1^2}{kT}} \cdot \exp\left\{-\frac{16\pi}{3}\left(\frac{\sigma v_1^{2/3}}{kT}\right)^3\left[\frac{1}{\ln S - Ky_1^e(S-1)}\right]^2\right\} \tag{A17}$$

*Manuscript received Apr. 2, 1990, and revision received July 6, 1990.*